Molecular Crystals and Liquid Crystals
Publication details, including instructions for authors and subscription information:
http://www.tandfonline.com/loi/gmcl20

Photoinduced Dewetting in Thin Films of Liquid Crystalline Dendritic Azobenzene Derivatives

Wenhan Li [a], Shusaku Nagano [a b], Koichiro Yonetake [c] & Takahiro Seki [a]

[a] Department of Molecular Design and Engineering, Graduate School of Engineering, Nagoya University, Furo-cho, Chikusa, Nagoya, Japan

[b] PRESTO, Japan Science and Technology Agency, Hon-cho, Kawaguchi, Japan

[c] Department of Organic Device Engineering, Graduate School of Science and Engineering, Yamagata University, Jonan, Yonezawa-shi, Yamagata, Japan

Version of record first published: 02 Aug 2012.

To cite this article: Wenhan Li , Shusaku Nagano , Koichiro Yonetake & Takahiro Seki (2012): Photoinduced Dewetting in Thin Films of Liquid Crystalline Dendritic Azobenzene Derivatives, Molecular Crystals and Liquid Crystals, 563:1, 112-120

To link to this article: http://dx.doi.org/10.1080/15421406.2012.689144

Mol. Cryst. Liq. Cryst., Vol. 563: pp. 112–120, 2012

ISSN: 1542-1406 print/1563-5287 online
DOI: 10.1080/15421406.2012.689144

Taylor & Francis
Taylor & Francis Group

Photoinduced Dewetting in Thin Films of Liquid Crystalline Dendritic Azobenzene Derivatives

WENHAN LI,[1] SHUSAKU NAGANO,[1,2] KOICHIRO YONETAKE,[3] AND TAKAHIRO SEKI[1,*]

[1]Department of Molecular Design and Engineering, Graduate School of Engineering, Nagoya University, Furo-cho, Chikusa, Nagoya, Japan
[2]PRESTO, Japan Science and Technology Agency, Hon-cho, Kawaguchi, Japan
[3]Department of Organic Device Engineering, Graduate School of Science and Engineering, Yamagata University, Jonan, Yonezawa-shi, Yamagata, Japan

We report in this paper photoinduced-dewetting phenomena observed for thin films (thickness < 100 nm) of a series of dendritic liquid crystalline materials with different spacer length (carbon number changing from n = 6 to 12) at their azobenzene units in the periphery. Spincast films of these dendrimers were prepared and exposed to UV light (365 nm) at various photon doses at room temperature. Atomic force microscopic observations of the dewetting forming process were performed step by step with increasing the UV illumination time for the dendrimer with the shortest spacer (n = 6). We observed how the dewetting bumps appeared from an initially flat spincast film and finally reached ca. eightfold of the initial film thickness. The dendrimer with n = 8 exhibited dewetting but the mass migration distance was significantly limited than that of n = 6. Dendrimers with longer spacer lengths (n = 10 and 12) did not exhibit dewetting behavior in the same conditions. These differences were discussed in terms of thermophysical properties of the materials.

Keywords Atomic force microscopy; azobenzene; dendrimers; liquid crystal; photoinduced dewetting

1. Introduction

Spontaneous formation of micro- and nano-patterns at the surface of soft matter induced by surface instability is a unique approach in the bottom-up fabrications. In the last three decades, dewetting of thin organic films from hard substrates has received significant attentions since polymers films are extensively applied to industrial applications. Pattern generation by dewetting provides low-cost solution processing techniques to pattern and orient organic crystals, which can be an important components for organic electronic devices [1].

Generally, dewetting describes the rupture of a thin liquid film on a substrate (either a liquid itself, or a solid) and the formation of droplets. Theoretically, due to long-range forces, in particular van der Waals forces for organic liquids, a flat thin liquid film is

*Address correspondence to Takahiro Seki, Department of Molecular Design and Engineering, Graduate School of Engineering, Nagoya University, Furo-cho, Chikusa, Nagoya 464-8603, Japan. E-mail: tseki@apchem.nagoya-u.ac.jp

thermodynamically unstable when its thickness becomes small. The films can dewet via heterogeneous nucleation and growth of dry patches, forming small clusters. They can also undergo spinodal dewetting, where thermal fluctuations of a critical capillary wavelength grow exponentially and determine the characteristic feature size [2–4]. The factor determining the spontaneous spreading and dewetting for a drop of oil placed on a liquid substrate (water here) with ambient gas, is the so-called spreading coefficient (S). When $S > 0$, the spontaneous spreading occurs, and if $S < 0$, dewetting occurs.

In most cases, annealing is adopted to proceed dewetting for a spin-cast film. Annealing a metastable film increases the mobility of the polymer chain molecules and dewetting takes place. However, little examples are known for photochemically induced dewetting that occurs isothermally. Cristofolini et al. [5] reported a UV light-induced dewetting for Langmuir–Blodgett (LB) films consisting of a liquid crystalline (LC) azobenzene-containing polyacrylate. UV irradiation induces the rod-like trans to the bent cis configuration, which reduces the molecular packing stability and thus soften the material. This situation increases the film instability on the surface. They found that the dewetting process (migrating distance) is strongly dependent on the film thickness that can be precisely controlled by the LB method.

In this paper, we report on the photoinduced-dewetting phenomenon observed for LC dendritic molecules shown in Fig. 1. The dendritic molecules possess the defined molecular

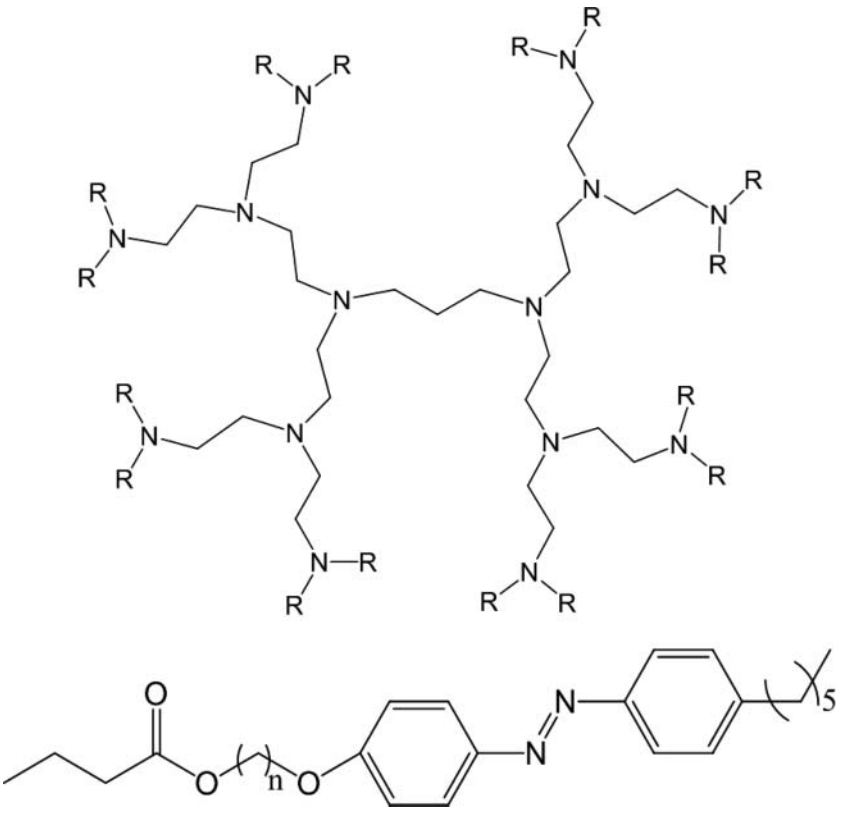

Figure 1. Chemical structure of amine-type dendrimers containing 16 azobenzene units in the periphery. Dn ($n = 6$, 8, 10, and 12).

mass and have no chance of chain entanglement among the molecules. Such systems eliminate the complexity and seem to be most suited for observation of the photoinduced-dewetting behavior. We will focus on (1) energy dose dependency on the dewetting behavior, and (2) the influence of the chemical structure of the dendrimers, which are discussed with the thermophysical properties.

2. Experimental

2.1. Materials

Figure 1 shows the molecular structure of dendrimers named from D6 to D12 used in our experiment. These compounds were synthesized in Yonetake laboratory in Yamagata University. The synthesis and characterizations of the dendrimer will be reported in due course. The differences between the four dendrimers are the length of their methylene spacer in the azobenzene unit. D6, D8, D10, and D12 have 6, 8, 10, and 12 methylene spacers, respectively.

2.2. Methods

2.2.1. Thermal Analysis. Differential scanning calorimeter (DSC) was carried out on a DSC Q20 MO-DSC-UV under helium purging gas (0.11 MPa) at a heating/cooling rate of 2°C min^{-1}.

2.2.2. Film Fabrication. Quarts substrates were first immersed in KOH-methanol mixture for several days for hydrophilic treatment, then washed by tap water and finally cleaned by ultrasonic treatments for 15 min while immersing in deionized water. Films were formed on the quarts substrates from chloroform solutions of D6 toD12 by spin-coating method. The spin speed was 3000 rpm. The whole process was carried out at room temperature. The initial thickness was ca. 95 nm for all samples. All films were prepared on a hydrophilic substrate.

2.2.3. Microscope Observation. The morphology of all films was observed by an atomic force microscope (AFM, Nanopics 2100, Seiko Instruments) using the damping mode. Original film thickness was also obtained using the same AFM instrument by creating and measuring a scratch on the film.

2.2.4. Light Irradiation. The films were later irradiated to a Xe-Hg UV lamp, Sanei-200s (nonpolarized) made by San-ei Electric through a 365 nm photo filter at room temperature. Incident light intensity was adjusted to 5 mw cm^{-2}, measured by a power meter. For D6 films, we exposed them to UV for 35 sec, 45 sec, 50 sec, 60 sec, 80 sec, and 100 sec, while D8, D10, and D12 film were equally exposed to UV for 50 sec.

2.2.5. Spectroscopic Measurements. UV-visible absorption spectra were taken on an Agilent 8453 diode array spectrometer.

3. Results and Discussion

3.1. UV-Visible Absorption Spectroscopy

Figure 2 shows the UV-visible absorption spectra of D6 in chloroform (dash-dotted line), of a spin-cast film before (solid line) and after (dash line) UV exposure. The absorption peak of the π-π^* long-axis transition of azobenzene in chloroform was positioned at 360 nm, while that of the spin-cast film was located at 320 nm. This fact indicates that the azobenzene unites form H-type aggregation partially in case of the spin-cast thin film state. The molecular orientation of the azobenzene units of the spin-cast film can be roughly estimated by the ratio of absorption intensities of the π-π^* long-axis transition of azobenzene (around 340 nm) to the π-π^* transition of phenyl (244 nm, often expressed as φ-φ^*) bands, since the direction of the π-π^* long-axis transition of azobenzene is directly dependent while that of the π-π^* transition of phenyl is essentially insensitive to the azobenzene orientation. The ratios of $A_{\pi\text{-}\pi^*}$ (azobenzene)/$A_{\pi\text{-}\pi^*}$ (phenyl) in chloroform solution and for the spin-cast film were 0.9 and 0.6. These spectral data indicates that the hydrophobic trans-azobenzene units have arranged mostly perpendicular to their substrates of the formed spin-cast films. For the film after UV exposure, the n-π^* of the cis-azobenzene absorption peak appeared at 450 nm. Obviously, the trans to cis photoisomerization underwent in the spin-cast film by the irradiation of UV light [6,7]. The grazing angle incidence X-ray measurements for a D12 film have revealed that the spin-cast film adopts the layer structure with a layer spacing of 3.7 nm [8], indicating that the layer consists of a bilayered smectic structure of perpendicularly oriented azobenzene units with respect to the substrate plane. It is reasonable to postulate that the same molecular packing is attained in the thin film of D6.

3.2. Photoinduced-Dewetting Behavior in D6

Unlike the rod-like trans-azobenzene, the molecular packing of the cis-azobenzene units are less ordered, which is known to soften the film after UV irradiation. The dewetting was

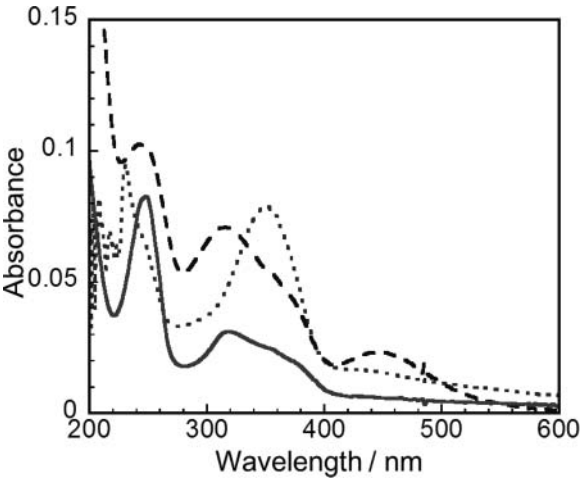

Figure 2. UV-visible absorption spectra of D6 in chloroform (doted line), in a spin-cast film before (solid line) and after (dashed line) UV exposure.

typically observed for D6. At room temperature, UV-irradiated azobenzene films turned to be a less stable liquid state. This effect is similar to what is frequently observed by annealing.

Figure 3 shows the topographical AFM images (100 μm $\times$ 100 μm) in the photoinduced-dewetting process of D6 films. In Fig. 4, the average height of the formed bumps is plotted against the increase of the energy dose. Interestingly, the height of the bumps formed by the dewetting were almost uniform regardless of the domain size. This situation rationalizes the profile in Fig. 4 to be reliable and meaningful. Initially, the film was flat with 95 nm thickness (Fig. 4a). The influence of UV photon dose on the dewetting behavior was examined for films in the same conditions. UV exposure energy was controlled by changing the duration of UV exposure with a fixed intensity of 5 mW cm^{-2}. The dewetting bumps appeared clearly and spontaneously after UV exposure of 175 mJ cm^{-2} (Fig. 4b, 5mW cm^{-2} for 35 sec irradiation). At 225 mJ cm^{-2}, continuous film domains no longer existed (Fig. 4c). With the exposed energy increased, the average morphological area of dewetting bumps shrank. Above 300 mJ cm^{-2}, the morphology was observed as round domains of diameters of some 10 μm, and virtually unchanged (Fig. 4d). However, the area of the domains became larger and the height increased considerably. When UV dose reached 400 mJ cm^{-2}, the morphological change finally became fixed (Fig. 4e). To our surprise, the height finally reached 771 nm at 400 mJ cm^{-2}, which corresponds to ca. eightfold of the initial thickness. Even by increasing the photon dose up to 600 mJ cm^{-2}, the morphology and the height of dewetting bumps remained unchanged (Fig. 4f). Figure 4 indicates a sigmoidal shape, suggesting that the dewetting process proceeds in a highly cooperative manner. The mass migration proceeded only when the UV was irradiated. The migration did not occur in the dark even if the film involves the cis-isomer. These results imply that the migration takes place only when the film is activated by UV irradiation.

3.3. Dependence of Dendrimer Structure

The dewetting behavior was found to be strongly dependent on the dendrimer structure. Both D6 and D8 showed dewetting behaviors at room temperature as shown in Fig. 5. But nothing happened morphologically for D10 and D12 when exposed to UV (data not shown). This discrepancy can be related to their thermophysical properties.

The DSC profiles from D6 to D12 in the trans-azobenzene form are displayed in Fig. 6. With increasing methylene spacers, the glass transition temperature (T_g), the transition temperature from SmB to SmA, and that from SmA to isotropic phase became higher accordingly. In the heating process, D6, D8, D10, and D12 showed the T_g at -8°C, 8°C, 14°C, and 17°C, respectively. The phase transition temperature from SmB to SmA enhanced as 33°C, 48°C, 65°C, and 77°C for D6, D8, D10, and D12, respectively. In the same way, the phase transition temperature from SmA to isotropic increased from 83°C, 100°C, 105°C, and 106°C for the same order. The dewetting is induced by an enrichment of the cis-isomers, therefore, the "real" thermal properties of the material that contributes the dewetting process cannot be the directly measured. However, the thermal data for the pure trans-azobenene state can be reasonably related to the dewetting behavior. Since the UV photoirradiation is achieved at room temperature for all cases, increasing the transition temperatures should impede the mass transfer upon dewetting. It seems that the molecular packing order of SmB (smectic LC phase possessing a hexatic order) in the tarns-azobenzene strongly governs whether the dewetting proceeds or not. The enthalpy change of the SmB to SmA phase ranging 60°C–70°C sharply became pronounced for

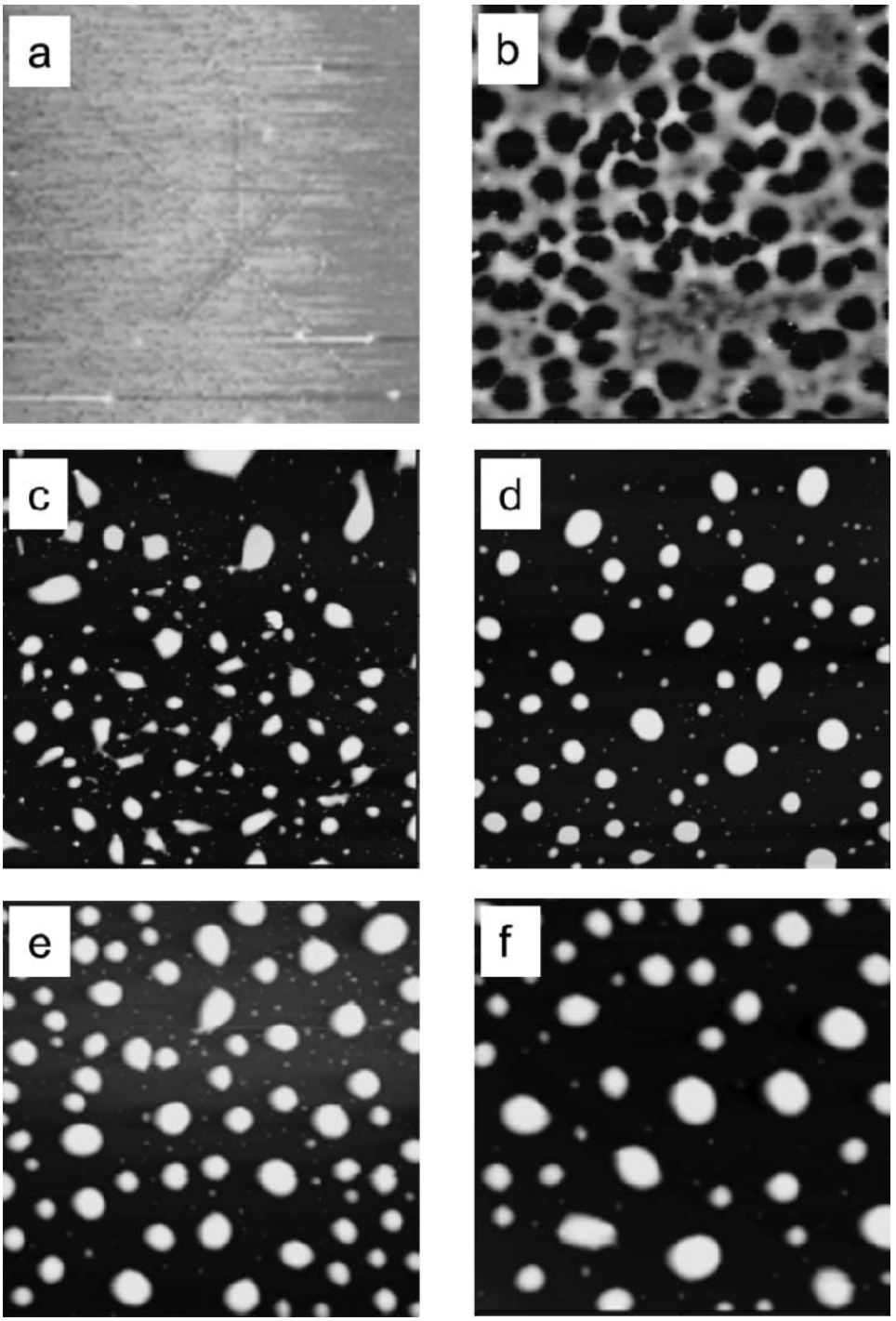

Figure 3. Dewetting morphologies (100 μm $\times$ 100 μm topographical AFM images) with UV irradiation period for D6 at room temperature. The images from a to f correspond to the irradiation period of 0s (initial film), 35 sec, 45 sec, 60 sec, 80 sec, and 100 sec, respectively, at the same UV intensity of 5 mW cm^{-2}.

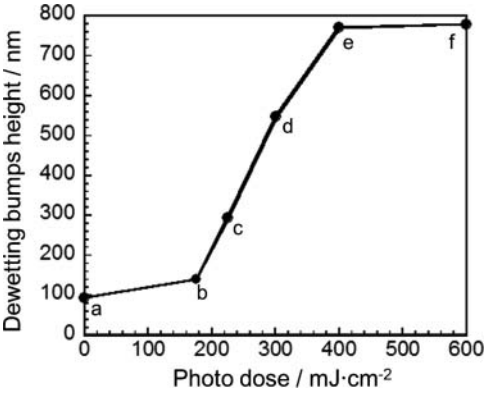

Figure 4. Height of the dewetting bumps versus UV photon dose on a D6 film which has an initial thickness of 95 nm (a). Plots from (a) to (f) are obtained from the AFM data shown in Fig. 3.

D10 and D12. In any event, the precise understanding needs the knowledge of the thermal properties of the film involving the cis-isomers, which will be the subject of future work.

As indicated in Fig. 5, the migration distance significantly differed from D6 to D8, which exhibits a large change in the bump size features after dewetting. Consequently, D8 provided much smaller domains (right), one order of magnitude smaller than those of D6. This can be also connected to the higher phase transition behavior of D8. The molecular mobility should be more suppressed in the D8 film due to the higher molecular packing order. Cristofolini et al. [5] discussed the migration distance with the change in film thickness. In the present case, the migration distance can be clearly related with the molecular structure.

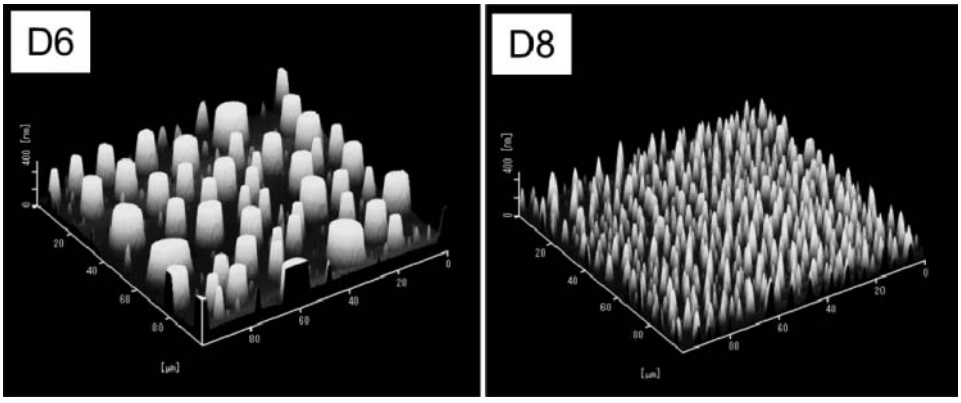

Figure 5. AFM images (100 μm $\times$ 100 μm area) of the bumps after dewetting for the D6 and D8 films at room temperature. Photon dose for both films are 250 mJ cm^{-2}.

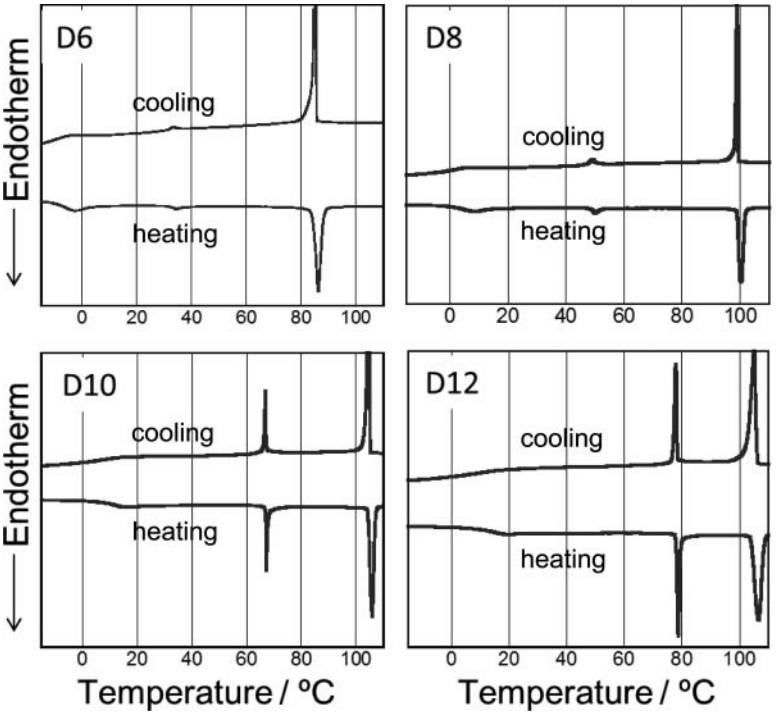

Figure 6. DSC curves of D6, D8, D10, and D12.

4. Conclusion

This work proposed a new photoinduced-dewetting process observed in dendritic azobenzene derivatives. UV light-induced dewetting occurred for compounds with shorter spacer length ($n = 6$ and 8) in the azobenzene unit. For longer spacer compounds ($n = 10$ and 12), the more ordered molecular packing seems to suppress the photoinduced dewetting and mass migration at room temperature as suggested by DSC measurements. In the case of D6 ($n = 6$), the dewetting proceeded after an induction period, and the migration and the height enhancement of the bumps occurred in the UV exposure range from 175 mJ cm^{-2} to 400 mJ cm^{-2}. This suggests that the mass migration occurs in a cooperative manner. The mass migration was very efficient and, to our surprise, the saturated height after dewetting reached ca. eightfold of the initial film thickness. Such high mobility of the material migration is probably due to the absence of chain entanglement which is characteristic in dendritic polymeric materials. We believe that these materials are fascinating to apply for photoinduced mass migration upon patterned irradiation using a photomask [6,7]. The approach in this direction is now underway and will be reported in due course.

Acknowledgment

This work was supported by the Grant-in-Aid a Grant-in-Aid for Scientific Research in Priority Areas "New Frontiers in Photochromism (No. 471)" and in basic research S (23225003) from the Ministry of Education, Culture, Sports, Science and Technology (MEXT), Japan.

References

[1] Menard, E., Meitl, M. A., Sun, Y., Park, J., Shir, D. J., Nam, Y., Jeon, S., & Rogers, J. A. (2007). *Chem. Rev.*, *107*, 1117.
[2] Xue, L., & Han, Y. (2011). *Prog. Polym. Sci.*, *36*, 269.
[3] Rosen, M. J. (2004). *Surfactants and Interfacial Phenomena* (3rd ed.), Hoboken: New Jersey.
[4] Karapanagiotis, I., & Gerberich, W. W. (2005). *Surface Sci.*, *594*, 192.
[5] Crustofolini, L., Fontana, M. P., Berzina, T., & Camorani P. (2003). *Mol. Cryst. Liq. Cryst.*, *398*, 11.
[6] Nishizawa, K., Nagano, S., & Seki, T. (2009). *Chem. Mater.*, *21*, 2624.
[7] Li, W., Nagano, S., & Seki, S. (2009). *New J. Chem.*, *33*, 1343.
[8] Lin, T., Nagano, S., & Seki, T., unpublished result.